


Timelike orbits around accelerating black holes

Mohammad Bagher Jahani Poshteh^{*}

*School of Physics, Institute for Research in Fundamental Sciences (IPM),
P.O. Box 19395-5531, Tehran 19538-33511, Iran*

 (Received 27 May 2022; accepted 8 August 2022; published 17 August 2022)

We study the geodesics of massive particles around an accelerating Schwarzschild black hole. We show that the radius of the innermost stable circular orbit and the angular momentum of a particle at this orbit decrease by increasing the acceleration. Apart from quantitative influence, the acceleration qualitatively changes the physics. We show that in accelerating black hole spacetime there exists an outermost stable circular orbit in flat, de Sitter, and anti-de Sitter backgrounds. Investigations of radial geodesics show that the acceleration acts like a repulsive force in the sense that test particles around accelerating black holes can move radially outward, unless there exists a large negative value of cosmological constant in the background to compensate the repulsive force. We also investigate the precession of perihelion of orbits around accelerating black holes. The precession would be larger compared to the nonaccelerating case. It is also shown that the precession in anti-de Sitter background could be opposite to the particle motion.

DOI: [10.1103/PhysRevD.106.044037](https://doi.org/10.1103/PhysRevD.106.044037)

I. INTRODUCTION

The study of the relativistic motion of particles in gravitational fields began shortly after the general theory of relativity was introduced [1–3]. In light of the investigations of lightlike geodesics, we have found many interesting phenomena, e.g., gravitational lensing [4–9] and black hole shadow [10–12]. These features are in common among black holes and naked singularities [13,14] and ultracompact objects [15,16].

The investigation of timelike geodesics around massive objects could help us understand the nature of the objects. In this paper we are interested in timelike geodesics in accelerating black hole spacetime. The motion of massive test particles around nonaccelerating black holes in general relativity has been thoroughly studied in [17]. In [18–20] fundamental frequencies of particles' motion around Kerr black holes have been investigated. Circular motions on equatorial plane around Kerr-Newman black holes and Kerr-Newman naked singularities are compared in [21]. In [22] null and timelike geodesics on the equatorial plane of a distorted Schwarzschild black hole are studied. In [23], for a class of naked singularity spacetimes, it has been shown that the perihelion precession can be in the opposite direction of a particle's motion. Precession of timelike bound orbits in Kerr spacetime has also been studied and it is found that the precession is positive [24].

Black holes can be pair produced on cosmic strings [25–27] as well as in a de Sitter [28–30] or magnetic field [31–33] background (see [34] for the black hole production

rate on the cosmic string in a de Sitter space with a background magnetic field). On the other, hand we might have primordial black holes become attached to cosmic strings in the early Universe [35]. All of these black holes will be accelerating (due to the tension of the cosmic string [35] and/or the force exerted by the positive cosmological constant and/or the magnetic field [34]).

Accelerating black holes could evolve to supermassive black holes [36] (see also [37]). However, if these black holes have played a role in structure formation, their velocity should be small [36], which means that the acceleration should be small. It has been speculated, from an observational point of view, that the black hole at the center of our Galaxy is connected to the cosmic string [38].

A study of null geodesics around accelerating black hole has recently attracted some attention [39–41]. The shadow of the accelerating black hole has been studied in [42,43]. On the other hand, thermodynamics of these black holes have been investigated in [44–46]. Near horizon symmetries of accelerating black holes have also been studied [47].

Accelerating black holes are described by the C metric. In [48], for the particles coaccelerating with the black hole at constant distance, null and timelike geodesics are found in the standard $\{x, y\}$ coordinates [49] as well as Weyl coordinates [50] and the coordinates adapted to the boost-rotation symmetry [51]. Generalization to the AdS C metric [52] and to the spinning C metric [53] have also been done. In [54], by studying the effective potential of test particles around the black hole, accessible regions for null/timelike geodesics are presented. Stability of geodesics is also discussed.

^{*}jahani@ipm.ir

The aim of this paper is to study the motion of massive particles in accelerating black hole spacetime with cosmological constant. We would like to study radial geodesics as well as the innermost stable circular orbit (ISCO) of particles around accelerating supermassive black holes. We would also like to investigate the perihelion precession of such orbits. In our examples we consider a nonrotating black hole with the same mass as the black hole at the center of Milky Way Galaxy, Sgr A*. We also use the orbital data of S2 star around Sgr A*. Considering the upper bound on the acceleration of supermassive black holes [36], we show that we can take S2 to be nearly on the equatorial plane of the accelerating black hole during one complete period.

The study of radial motion of test particles in accelerating black hole spacetime shows that these particles can move radially outward. This means that accelerating black holes exert some sort of repulsive force on test particles. We also find the interesting result that there exists an upper bound on the radius of stable circular orbits around the accelerating black hole. These features are in common among accelerating black holes and black holes in de Sitter spacetime.

We also investigate the precession of orbits around accelerating black holes. We show that the precession of perihelion is larger for larger values of black hole acceleration. However, for black holes in anti-de Sitter (AdS) background, the precession can be negative (the orbit precesses in the opposite direction of the motion).

The outline of our paper is as follows. In the next section we present the Lagrangian of motion on a plane perpendicular to the direction of acceleration (equatorial plane) and study the radial motion on this plane. Stable circular orbits on the equatorial plane are studied in Sec. III. In Sec. IV we study the precession of the orbits. We conclude our paper in Sec. V. We work in geometric units where $G = c = 1$ and use mostly positive signatures for the spacetime metric.

II. RADIAL MOTIONS ON EQUATORIAL PLANE

It has been shown in [36] that the velocity of supermassive black holes connected to the cosmic string should be less than 100 km/s so that they could be captured by galaxies during the structure formation. This, in turn, constrains tension of the cosmic string to $\mu \lesssim 10^{-19} \sqrt{M/M_\odot}$, where M is the mass of supermassive black hole connected to the cosmic string. For the black hole at the center of our Galaxy, with $M_{\text{Sgr A}^*} \simeq 4.23 \times 10^6 M_\odot$ [55], the tension of the cosmic string attached to it would be $\mu \lesssim 2.06 \times 10^{-16}$. Therefore, we find from Newton's second law, $\mu = \alpha M_{\text{Sgr A}^*}$, that the acceleration is $\alpha \lesssim 3.29 \times 10^{-26} \text{ m}^{-1}$.

The orbital period of S2 star around Sgr A* is about 16 years [56,57]. We take the acceleration of Sgr A* to be $\alpha = 10^{-26} \text{ m}^{-1}$ —this is about the largest value allowed by

[36]. Assuming the initial velocity of the black hole to be zero, the displacement of the black hole during the period of S2 is $2.29 \times 10^8 \text{ m}$. This is much smaller than the Schwarzschild radius of the black hole that is of the order of 10^{10} m . Therefore, we can assume that, if S2 starts its period near the equatorial plane of the black hole, it will remain near this plane during one period of the orbit around the slowly accelerating black hole.

The spacetime around uniformly accelerating black holes is described by the C metric.¹ The (A)dS C metric has been studied in, for example, [29,59–62]. For a black hole of mass m and uniform acceleration α , in a background spacetime with cosmological constant Λ , the metric can be written in the following form [63]:

$$ds^2 = \frac{1}{(1 + \alpha r \cos \theta)^2} \left[-Q(r) dt^2 + \frac{dr^2}{Q(r)} + \frac{r^2 d\theta^2}{P(\theta)} + P(\theta) r^2 \sin^2 \theta d\phi^2 \right], \quad (1)$$

where

$$Q(r) = (1 - \alpha^2 r^2) \left(1 - \frac{2m}{r} \right) - \frac{\Lambda}{3} r^2, \\ P(\theta) = 1 + 2\alpha m \cos \theta. \quad (2)$$

The coordinate t ranges over all of \mathbb{R} and $0 \leq \theta \leq \pi$. The periodicity of ϕ is $-C_0\pi \leq \phi \leq C_0\pi$. One can choose C_0 so as to eliminate the conical singularity at one of the poles. We take $C_0 = (1 + 2\alpha m)^{-1}$ to eliminate the singularity at $\theta = 0$ [54].²

We would like to study the geodesics on the equatorial plane of the accelerating black holes. We assume that the direction of acceleration is perpendicular to this plane. On the equatorial plane the metric (1) reduces to

$$ds^2 = -Q dt^2 + \frac{dr^2}{Q} + r^2 d\theta^2 + r^2 d\phi^2, \quad (3)$$

with the metric function given by Eq. (2).

The metric function Q has been plotted in Fig. 1. We have taken some large values of acceleration and cosmological constant so that we could better illustrate the behavior of the metric function in different cases. For the case of flat and de Sitter backgrounds the metric function has two zeros for positive r and has a maximum

¹This spacetime is of algebraic type D. It has been proved in [58] that vacuum type D spacetimes admit Killing and Killing-Yano tensors if (and only if) they are without acceleration.

²Setting $C_0 = (1 + 2\alpha m)^{-1}$, on the other hand, eliminates the singularity at $\theta = 0$ [54]. For other choices of C_0 neither the singularity at $\theta = 0$ nor the one at $\theta = \pi$ would be eliminated and one has cosmic strings at both poles.

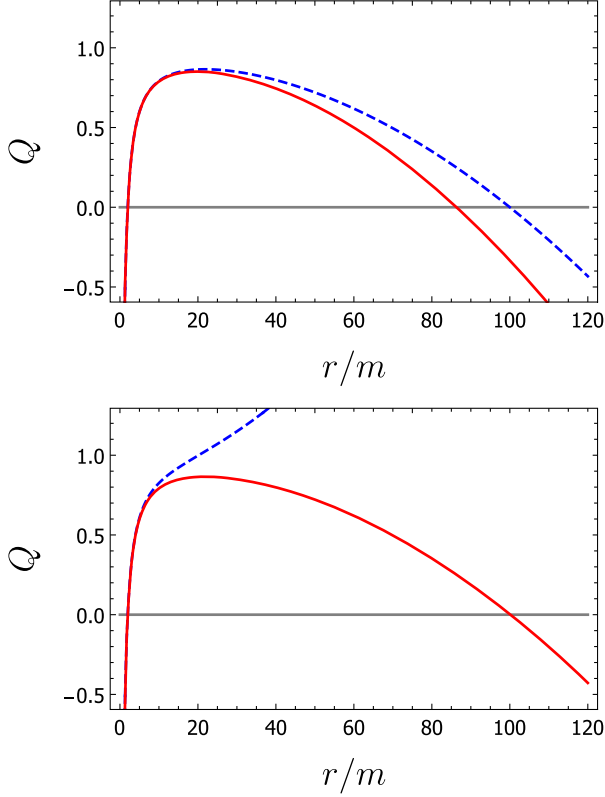


FIG. 1. Top: The metric function of an accelerating black hole in flat (dashed blue plot) and de Sitter with $m^2\Lambda = 10^{-4}$ (solid red plot) backgrounds. Bottom: The metric function of an accelerating black hole in anti-de Sitter background with $m^2\Lambda = -10^{-3}$ (dashed blue plot) and $m^2\Lambda = -10^{-6}$ (solid red plot). We have taken $m\alpha = 10^{-2}$.

between them. The behavior of the metric function in the case of the anti-de Sitter background is more interesting. For $\Lambda > -3\alpha^2$ there are two zeros for positive r ; however, if $\Lambda < -3\alpha^2$ there would be only one zero and the metric function goes to $+\infty$ as r increases.³

The region between the two zeros of Q —one associated to the event horizon of the black hole, the other to the acceleration horizon—is the domain of outer communication in which $Q > 0$. For $\Lambda < -3\alpha^2$ this domain contains any radius larger than the radius of the black hole’s event horizon. The motion of the test body around the black hole is in the region of outer communication. Therefore we only consider the range of r which is in the domain of outer communication.

The Lagrangian governing the geodesic motion is $2\mathcal{L} = g_{\gamma\sigma}\dot{x}^\gamma\dot{x}^\sigma = -\mu^2$, where μ is the rest mass of the infalling particle and the dot, for timelike geodesics, represents differentiation with respect to the proper time

³For $\Lambda > -3\alpha^2$ there is a maximum between two zeros of the metric function. As $\Lambda \rightarrow (-3\alpha^2)^+$ the point at which the maximum appears goes to $+\infty$.

(for a detailed study of timelike geodesics in Schwarzschild and Kerr background see [17]). Using the metric (3) the Lagrangian on equatorial plane would be

$$\mathcal{L} = \frac{1}{2} \left(-Q\dot{t}^2 + \frac{\dot{i}^2}{Q} + r^2\dot{\phi}^2 \right). \quad (4)$$

The canonical momenta $p_t = -\frac{\partial\mathcal{L}}{\partial\dot{t}}$ and $p_\phi = \frac{\partial\mathcal{L}}{\partial\dot{\phi}}$ are conserved because of the symmetry of the metric, i.e., $\dot{p}_t = -\frac{\partial\mathcal{L}}{\partial t} = 0$ and $\dot{p}_\phi = \frac{\partial\mathcal{L}}{\partial\phi} = 0$. They are the energy and angular momentum of the infalling particle and can be found to be

$$E = p_t = Q\dot{t}, \quad L_z = p_\phi = r^2\dot{\phi}. \quad (5)$$

We note here that if the acceleration has a component parallel to the equatorial plane which is of the same order or larger than the perpendicular component, then the third component of the angular momentum is no longer a constant of motion. In this case geodesic equations cannot be analytically integrated. By using these quantities we can rewrite Eq. (4) as

$$\dot{i}^2 = \tilde{E}^2 - Q \left[1 + \frac{\tilde{L}_z^2}{r^2} \right], \quad (6)$$

where \tilde{E} and \tilde{L}_z are, respectively, the energy and angular momentum per unit rest mass and the dot now represents differentiation with respect to proper time per unit rest mass. Note also that the second term on the right-hand side of Eq. (6),

$$\tilde{V} = Q \left[1 + \frac{\tilde{L}_z^2}{r^2} \right], \quad (7)$$

is the effective potential.

Now we consider radial motion in accelerating black hole spacetime.⁴ For radial geodesics we have $\tilde{L}_z = 0$. Therefore, Eq. (6) reduces to

$$\dot{i}^2 = \tilde{E}^2 - Q. \quad (8)$$

If a test particle is falling from rest at r_0 we find $\tilde{E}^2 = Q(r_0)$.

For the nonaccelerating Schwarzschild black hole in anti-de Sitter background it has been shown that the test particle always plunges into the black hole [64]. This is due to the attractive force generated by the negative cosmological constant. However, for the nonaccelerating Schwarzschild black hole in de Sitter background, it is known that the test particle can move radially outward/inward if r_0 is larger/smaller than a specific value [65].

⁴For a black hole accelerating in the z direction, we consider radial motion in the x - y plane.

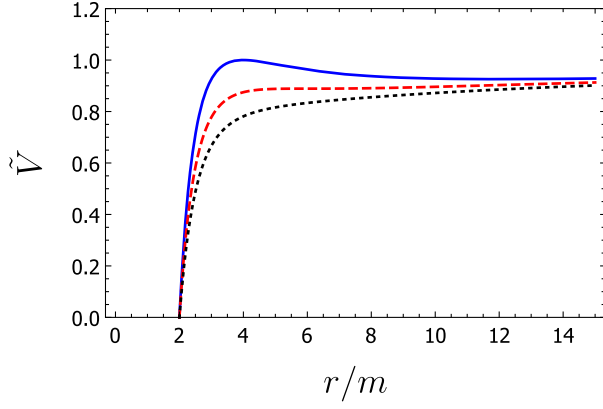


FIG. 2. The effective potential for different values of angular momentum in the region near the black hole horizon. We have taken $m\alpha = 10^{-26}$, $m^2\Lambda = 10^{-52}$, and $\tilde{L}_z = 3m$ (dotted black plot), $\tilde{L}_z = \tilde{L}_{z,\text{ISCO}} \approx 3.4641m$ (dashed red plot), and $\tilde{L}_z = 4m$ (solid blue plot). The maximum and minimum of the solid blue plot are, respectively, at $r \approx 4m$ and $r \approx 12m$. The inflection point of the dashed red plot is at $r \approx 6m$.

The acceleration of the test particle which is at rest at r_0 is given by [65]

$$\ddot{r} = \frac{Q'(r)[\dot{r}^2 - Q(r_0)]}{2Q(r)}. \quad (9)$$

For $\Lambda > -3\alpha^2$ the metric function Q has two zeros at positive r (see Fig. 1). Let us denote the smaller root by r_+ and the larger one by r_{++} . Between these two roots the metric function has a maximum at r_M . Suppose a test particle starts its motion at r_0 . For $r_+ < r_0 < r_M$ the slope of the metric function is positive; therefore, the initial acceleration $\dot{r} = -Q'(r_0)/2$ is negative. This means that the test particle plunges into the black hole. For $r_M < r_0 < r_{++}$, however, the acceleration is positive and the test particle moves radially outward. On the other hand, in anti-de Sitter background with $\Lambda < -3\alpha^2$, the test particle always plunges into the event horizon.

Therefore we find that acceleration acts like a positive cosmological constant. Similarity between a positive cosmological constant and cosmic strings has already been claimed in the context of black hole pair production in the author's earlier work [34]. We also see that a negative cosmological constant can compensate the acceleration ($\Lambda = -3\alpha^2$ completely compensates the effect of α).

III. STABLE CIRCULAR ORBITS

Here we consider the circular geodesics for which $\tilde{L}_z \neq 0$. We have plotted the effective potential in Fig. 2 for different values of the angular momentum in the region near the event horizon of the black hole (we take approximately the observed value of the cosmological constant, $\Lambda \simeq 10^{-52} \text{ m}^{-2}$ [66]). In this region, we see that for \tilde{L}_z

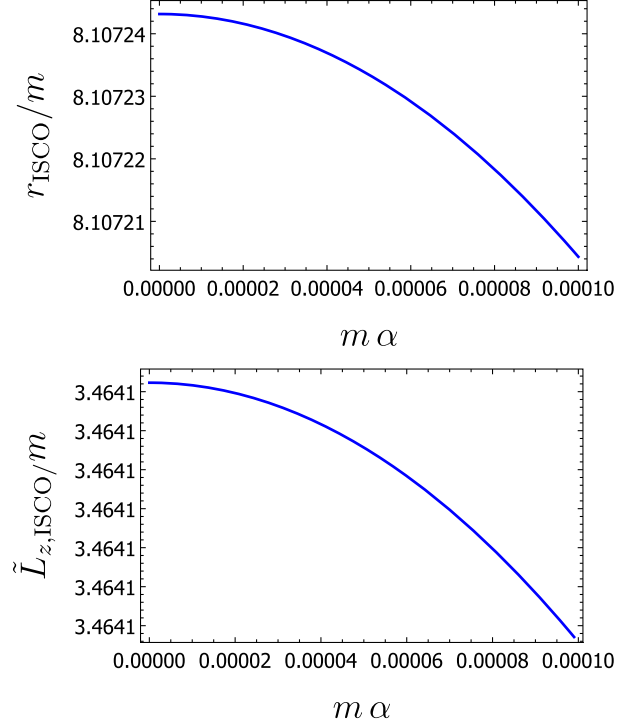


FIG. 3. Top: The radius of ISCO as a function of the acceleration of the black hole. Bottom: The angular momentum of the particle on ISCO. We have taken $m^2\Lambda = 10^{-52}$.

slightly above $\tilde{L}_{z,\text{ISCO}}$ there are a minimum and a maximum in the plot of the potential which are associated to stable and unstable circular orbits, respectively. The minimum gets closer to the black hole as \tilde{L}_z decreases. For $\tilde{L}_z = \tilde{L}_{z,\text{ISCO}}$ we have the ISCO which is at the inflection point of the effective potential.

We find that the radius of ISCO and the angular momentum of the particle at this orbit depends on the acceleration. In Fig. 3, using numerical techniques, we have plotted the radius of ISCO and the angular momentum at ISCO as a function of the acceleration. We see that both of them decrease by increasing the acceleration. This means that if the black hole is accelerating, the infalling particle can orbit on a stable circular orbit around the hole with a smaller radius and angular momentum.

For nonaccelerating black holes, it is known that there exists an outermost stable circular orbit (OSCO) in a background spacetime with a positive cosmological constant [67,68]. We have found that, for accelerating black holes, OSCO exists for flat and AdS backgrounds as well as in dS spacetime. This point has been presented in Fig. 4. Let us call the region in which the OSCO takes place as the far region. We see that for \tilde{L}_z slightly below $\tilde{L}_{z,\text{OSCO}}$ there are a minimum and a maximum in the plot of the potential which are, respectively, associated to stable and unstable circular orbits. The minimum goes away from the black hole as \tilde{L}_z increases. For $\tilde{L}_z = \tilde{L}_{z,\text{OSCO}}$ we have the OSCO which is at the inflection point of the effective potential.

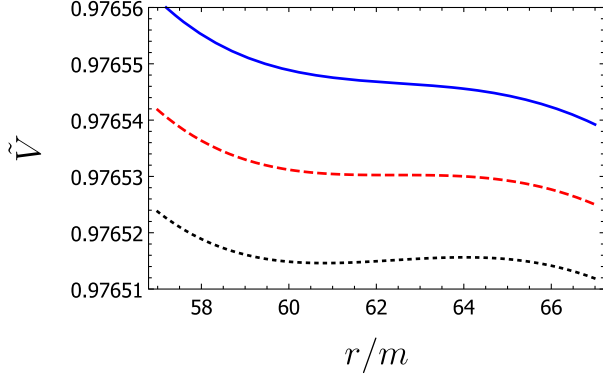


FIG. 4. The effective potential for different values of angular momentum in the region far from the black hole horizon. We have taken $m\alpha = 10^{-3}$, $\Lambda = 0$, and $\tilde{L}_z = 7.05800m$ (dotted black plot), $\tilde{L}_z = \tilde{L}_{z,\text{OSCO}} \approx 7.06232m$ (dashed red plot), and $\tilde{L}_z = 7.06700m$ (solid blue plot).

In Fig. 5 we see that the radius of OSCO and the angular momentum of the particle at this orbit decrease by increasing the acceleration. We also note that there is a critical value of acceleration for which OSCO and ISCO would be on top of each other. (For the value of the cosmological constant taken in Figs. 3 and 5 the critical acceleration is $m\alpha \simeq 1.61466 \times 10^{-2}$.)

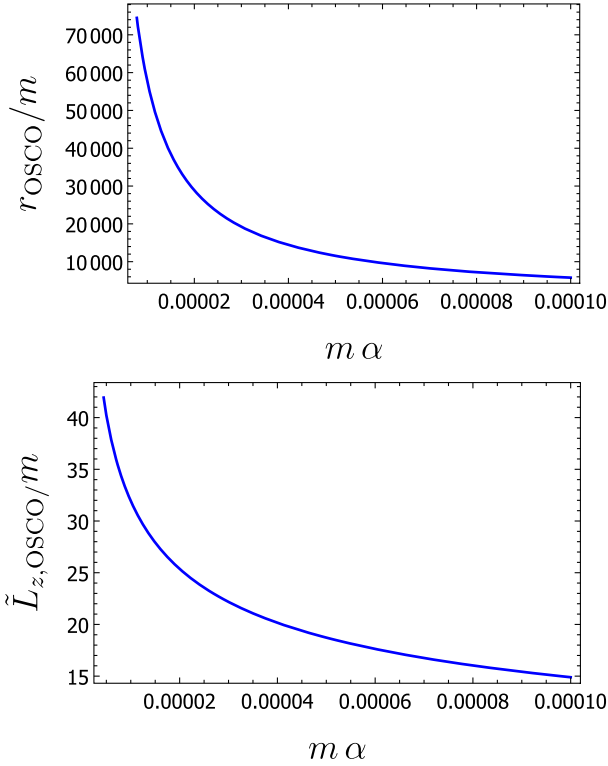


FIG. 5. Top: The radius of OSCO as a function of the acceleration of the black hole. Bottom: The angular momentum of the particle on OSCO. We have taken $m^2\Lambda = 10^{-52}$.

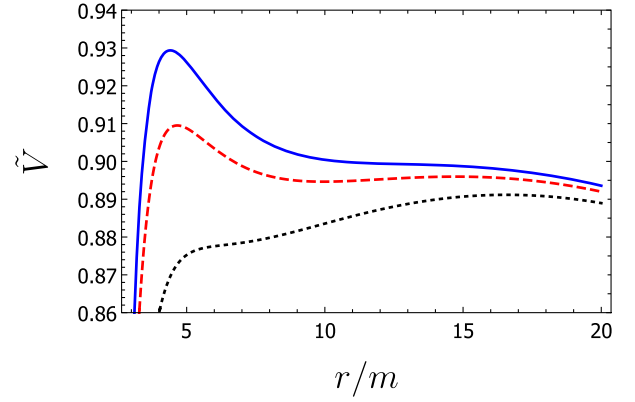


FIG. 6. The effective potential for different values of angular momentum in the near and far regions from the black hole horizon. We have taken $m\alpha = 10^{-2}$, $\Lambda = 0$, and $\tilde{L}_z = 3.4m < \tilde{L}_{z,\text{ISCO}}$ (dotted black plot), $\tilde{L}_{z,\text{ISCO}} < \tilde{L}_z = 3.6m < \tilde{L}_{z,\text{OSCO}}$ (dashed red plot), and $\tilde{L}_z = 3.7m > \tilde{L}_{z,\text{OSCO}}$ (solid blue plot). Qualitatively similar behaviors take place in the de Sitter and anti-de Sitter background as well.

Behavior of the potential in both the near and the far regions is presented in Fig. 6. For the case in which $\tilde{L}_z < \tilde{L}_{z,\text{ISCO}}$ ($\tilde{L}_z > \tilde{L}_{z,\text{OSCO}}$) the potential has a maximum in the far (near) region. If the energy of the particle coming from infinity is larger than the maximum value of the potential it will plunge into the black hole. The case in which $\tilde{L}_{z,\text{ISCO}} < \tilde{L}_z < \tilde{L}_{z,\text{OSCO}}$ is more interesting and has been presented in the middle (dashed red) plot of Fig. 6. In this case there are two maxima at r_{max_1} and r_{max_2} [assuming $r_{\text{max}_1} < r_{\text{max}_2}$ and $\tilde{V}(r_{\text{max}_1}) > \tilde{V}(r_{\text{max}_2})$] and one minimum between them at r_{min} .

Ignoring the particles confining to $r < r_{\text{max}_1}$, depending on the energy of the particle, the following cases could happen:

- (i) For a particle approaching the black hole, if the energy satisfies $\tilde{E}^2 > \tilde{V}(r_{\text{max}_1})$, the particle would plunge into the black hole.
- (ii) If $\tilde{V}(r_{\text{max}_2}) < \tilde{E}^2 < \tilde{V}(r_{\text{max}_1})$, the particle reaches a minimum radius in the range $r_{\text{max}_1} < r < r_{\text{min}}$ and then escapes to infinity.
- (iii) If $\tilde{V}(r_{\text{min}}) < \tilde{E}^2 < \tilde{V}(r_{\text{max}_2})$, and if the particle is coming from infinity, it reaches a minimum radius of $r > r_{\text{max}_2}$. The other possibility is that the particle rotates around the black hole in a bound orbit with radius $r_{\text{max}_1} < r < r_{\text{max}_2}$.
- (iv) If $\tilde{E}^2 < \tilde{V}(r_{\text{min}})$ the particles coming from infinity would reach a minimum at $r > r_{\text{max}_2}$ [here r is larger than the case in which $\tilde{V}(r_{\text{min}}) < \tilde{E}^2 < \tilde{V}(r_{\text{max}_2})$] and then escape to infinity.

Also if $\tilde{E}^2 = \tilde{V}(r_{\text{max}_1})$ or $\tilde{E}^2 = \tilde{V}(r_{\text{max}_2})$ the particle will rotate the black hole on an unstable circular orbit, and if $\tilde{E}^2 = \tilde{V}(r_{\text{min}})$ the particle will rotate the black hole on a stable circular orbit.

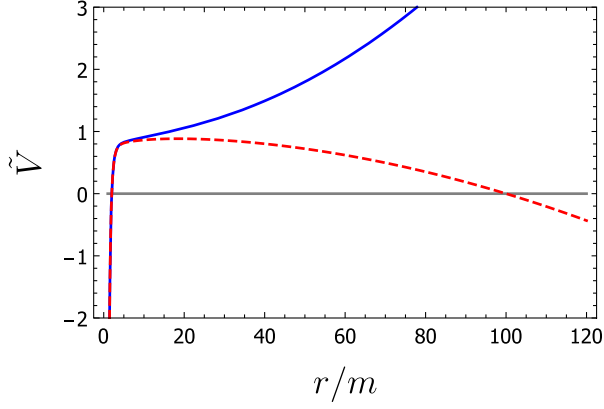


FIG. 7. The effective potential for $m\alpha = 10^{-6}$ and $m^2\Lambda = -10^{-3}$ (solid blue plot) and $m\alpha = 10^{-2}$ and $m^2\Lambda = -10^{-10}$ (dashed red plot). The solid blue plot satisfies $\Lambda < -3\alpha^2$, while for the dashed red plot $\Lambda > -3\alpha^2$. We have taken $\tilde{L}_z = 3m$ in both plots.

We also note that for $\Lambda < -3\alpha^2$ the potential goes to $+\infty$ as r increases. However for $\Lambda > -3\alpha^2$ (whether in de Sitter, flat, or anti-de Sitter backgrounds) the potential goes to $-\infty$ as r increases. These points have been illustrated in Fig. 7.

IV. PRECESSION OF PERIHELION

In this section we investigate the precession of perihelion for orbits around accelerating black holes. Equation (4) can be written as

$$\left(\frac{dr}{d\phi}\right)^2 = \frac{r^4 \tilde{E}^2}{\tilde{L}_z^2} - \frac{Qr^4}{\tilde{L}_z^2} - Qr^2. \quad (10)$$

At the perihelion and aphelion we have $dr/d\phi = 0$. If we denote the radius of the perihelion and aphelion, respectively, by r_p and r_a , we can write the energy and angular momentum per unit rest mass as

$$\tilde{E}^2 = \frac{Q(r_a)Q(r_p)(r_p^2 - r_a^2)}{Q(r_a)r_p^2 - Q(r_p)r_a^2}, \quad (11)$$

$$\tilde{L}_z^2 = \frac{r_a^2 r_p^2 [Q(r_p) - Q(r_a)]}{Q(r_a)r_p^2 - Q(r_p)r_a^2}. \quad (12)$$

As we mentioned earlier, the periodicity of ϕ is $2C_0\pi$, with $C_0 = (1 + 2\alpha m)^{-1}$. Therefore, the precession can be found, by using Eq. (10), as

$$\begin{aligned} \Delta\phi &= 2[\phi(r_a) - \phi(r_p)] - 2(1 + 2\alpha m)^{-1}\pi \\ &= 2 \int_{r_p}^{r_a} \frac{dr}{\sqrt{\frac{r^4 \tilde{E}^2}{\tilde{L}_z^2} - \frac{Qr^4}{\tilde{L}_z^2} - Qr^2}} - 2(1 + 2\alpha m)^{-1}\pi, \end{aligned} \quad (13)$$

where \tilde{E}^2 and \tilde{L}_z^2 are given by Eqs. (11) and (12).

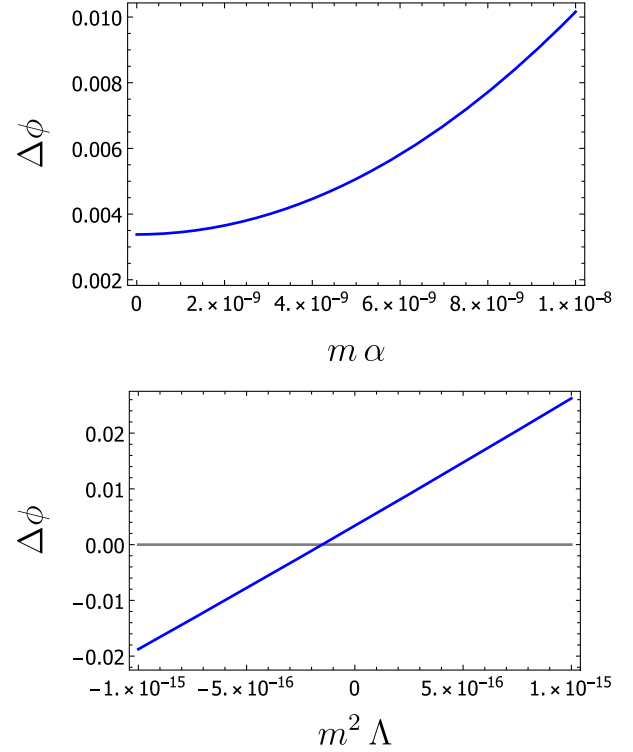


FIG. 8. Top: Precession of perihelion as a function of the acceleration. We have taken $\Lambda = 0$. Bottom: Precession of perihelion as a function of the cosmological constant. We have taken $\alpha = 0$.

The radius of the perihelion and aphelion are related to the eccentricity e and semimajor axis a of the orbit through $r_p = (1 - e)a$ and $r_a = (1 + e)a$. As an example we take the semimajor axis and eccentricity of S2 in its orbit around Sgr A*. They are $a = 1.543 \times 10^{14}$ m and $e = 0.88$ [69].

In the top panel of Fig. 8 we have plotted the precession (13) as a function of acceleration for S2. We see that the precession angle increases by increasing the acceleration of the central black hole. Also in the bottom panel of Fig. 8 we see that the precession increase by increasing the cosmological constant. It is very interesting that the precession angle is negative for $m^2\Lambda \lesssim -1.51363 \times 10^{-16}$.

V. CONCLUDING REMARKS

We have studied the geodesics of massive particles on equatorial plane of accelerating black holes. We have only considered the component of the acceleration which is perpendicular to the plane of the particle motion. If the component parallel to this plane is considerably large, then the angular momentum of the particle is no longer a constant of motion and we would only have one constant of motion (the energy). In that case the geodesic equations cannot be solved analytically.

We have found several new and interesting results. The study of radial geodesics and stable circular orbits around an

accelerating black hole show that there exists some sort of similarity between accelerating black holes and black holes in de Sitter background. The radially outward motion of test particles in accelerating black hole spacetime points out that acceleration, like a positive cosmological constant, generates a repulsive force. (However, in the case of de Sitter space, the “cosmic acceleration” is spherically symmetric, whereas here in acceleration is in the z direction.) Another similarity is the existence of OSCO in accelerating black hole spacetimes which also exists for particles orbiting a black hole in de Sitter background.

We have found that the precession of perihelion is larger around an accelerating black hole. It is also shown that in

anti-de Sitter background the precession can be negative. We postpone a detailed study of the precession in anti-de Sitter background to a future work. It would also be very interesting to study the timelike geodesics around rotating accelerating black holes.

ACKNOWLEDGMENTS

We are grateful to M.M. Sheikh-Jabbari for reading several prepublication versions of this paper and providing us with useful comments. We also acknowledge the support of Iran Science Elites Federation and the hospitality of the University of Guilan.

-
- [1] A. Einstein, The foundation of the general theory of relativity, *Ann. Phys. (Berlin)* **354**, 769 (1916).
- [2] F.W. Dyson, A. S. Eddington, and C. Davidson, A determination of the deflection of light by the Sun’s gravitational field, from observations made at the total eclipse of May 29, 1919, *Phil. Trans. R. Soc. A* **220**, 291 (1920).
- [3] A. Einstein, Lens-like action of a star by the deviation of light in the gravitational field, *Science* **84**, 506 (1936).
- [4] P. Schneider, J. Ehlers, and E. E. Falco, *Gravitational Lenses* (Springer, New York, 1992).
- [5] C. Darwin, The gravity field of a particle, *Proc. R. Soc. A* **249**, 180 (1959).
- [6] C. Darwin, The gravity field of a particle. II, *Proc. R. Soc. A* **263**, 39 (1961).
- [7] M. B. Jahani Poshteh and R. B. Mann, Gravitational lensing by black holes in Einsteinian cubic gravity, *Phys. Rev. D* **99**, 024035 (2019).
- [8] K. S. Virbhadra and G. F. R. Ellis, Schwarzschild black hole lensing, *Phys. Rev. D* **62**, 084003 (2000).
- [9] K. S. Virbhadra, Relativistic images of Schwarzschild black hole lensing, *Phys. Rev. D* **79**, 083004 (2009).
- [10] J.L. Synge, The escape of photons from gravitationally intense stars, *Mon. Not. R. Astron. Soc.* **131**, 463 (1966).
- [11] R. A. Hennigar, M. B. Jahani Poshteh, and R. B. Mann, Shadows, signals, and stability in Einsteinian cubic gravity, *Phys. Rev. D* **97**, 064041 (2018).
- [12] K. Akiyama, A. Alberdi, W. Alef, K. Asada, R. Azulay, A.-K. Baczkó, D. Ball, M. Baloković, J. Barrett, D. Bintley *et al.*, First M87 event horizon telescope results. IV. Imaging the central supermassive black hole, *Astrophys. J. Lett.* **875**, L4 (2019).
- [13] K. S. Virbhadra and G.F. Ellis, Gravitational lensing by naked singularities, *Phys. Rev. D* **65**, 103004 (2002).
- [14] A. B. Joshi, D. Dey, P. S. Joshi, and P. Bambhaniya, Shadow of a naked singularity without photon sphere, *Phys. Rev. D* **102**, 024022 (2020).
- [15] P. V. Cunha and C. A. Herdeiro, Shadows and strong gravitational lensing: A brief review, *Gen. Relativ. Gravit.* **50**, 42 (2018).
- [16] R. Shaikh, P. Banerjee, S. Paul, and T. Sarkar, Analytical approach to strong gravitational lensing from ultracompact objects, *Phys. Rev. D* **99**, 104040 (2019).
- [17] S. Chandrasekhar, *The Mathematical Theory of Black Holes* (Oxford University Press, New York, 1998), Vol. 69.
- [18] D. C. Wilkins, Bound geodesics in the Kerr metric, *Phys. Rev. D* **5**, 814 (1972).
- [19] K. Glampedakis and D. Kennefick, Zoom and whirl: Eccentric equatorial orbits around spinning black holes and their evolution under gravitational radiation reaction, *Phys. Rev. D* **66**, 044002 (2002).
- [20] R. Fujita and W. Hikida, Analytical solutions of bound timelike geodesic orbits in Kerr spacetime, *Classical Quantum Gravity* **26**, 135002 (2009).
- [21] D. Pugliese, H. Quevedo, and R. Ruffini, Equatorial circular orbits of neutral test particles in the Kerr-Newman spacetime, *Phys. Rev. D* **88**, 024042 (2013).
- [22] A. A. Shoom, C. Walsh, and I. Booth, Geodesic motion around a distorted static black hole, *Phys. Rev. D* **93**, 064019 (2016).
- [23] P. Bambhaniya, A. B. Joshi, D. Dey, and P. S. Joshi, Timelike geodesics in naked singularity and black hole spacetimes, *Phys. Rev. D* **100**, 124020 (2019).
- [24] P. Bambhaniya, D. N. Solanki, D. Dey, A. B. Joshi, P. S. Joshi, and V. Patel, Precession of timelike bound orbits in Kerr spacetime, *Eur. Phys. J. C* **81**, 205 (2021).
- [25] S. W. Hawking and S. F. Ross, Pair Production of Black Holes on Cosmic Strings, *Phys. Rev. Lett.* **75**, 3382 (1995).
- [26] D. M. Eardley, G. T. Horowitz, D. A. Kastor, and J. H. Traschen, Breaking Cosmic Strings Without Monopoles, *Phys. Rev. Lett.* **75**, 3390 (1995).
- [27] A. Ashoorioon and R. B. Mann, Black holes as beads on cosmic strings, *Classical Quantum Gravity* **31**, 225009 (2014).
- [28] F. Mellor and I. Moss, Black holes and quantum wormholes, *Phys. Lett. B* **222**, 361 (1989).
- [29] R. B. Mann and S. F. Ross, Cosmological production of charged black hole pairs, *Phys. Rev. D* **52**, 2254 (1995).

- [30] O. J. C. Dias and J. P. S. Lemos, Pair creation of de Sitter black holes on a cosmic string background, *Phys. Rev. D* **69**, 084006 (2004).
- [31] D. Garfinkle and A. Strominger, Semiclassical Wheeler wormhole production, *Phys. Lett. B* **256**, 146 (1991).
- [32] S. W. Hawking, G. T. Horowitz, and S. F. Ross, Entropy, area, and black hole pairs, *Phys. Rev. D* **51**, 4302 (1995).
- [33] F. Dowker, J. P. Gauntlett, S. B. Giddings, and G. T. Horowitz, On pair creation of extremal black holes and Kaluza-Klein monopoles, *Phys. Rev. D* **50**, 2662 (1994).
- [34] A. Ashoorioon and M. B. Jahani Poshteh, Black hole pair production on cosmic strings in the presence of a background magnetic field, *Phys. Lett. B* **816**, 136224 (2021).
- [35] A. Vilenkin, Cosmic strings and domain walls, *Phys. Rep.* **121**, 263 (1985).
- [36] A. Vilenkin, Y. Levin, and A. Gruzinov, Cosmic strings and primordial black holes, *J. Cosmol. Astropart. Phys.* **11** (2018) 008.
- [37] A. Gußmann, Polarimetric signatures of the photon ring of a black hole that is pierced by a cosmic axion string, *J. High Energy Phys.* **08** (2021) 160.
- [38] M. R. Morris, J.-H. Zhao, and W. Goss, A nonthermal radio filament connected to the galactic black hole?, *Astrophys. J. Lett.* **850**, L23 (2017).
- [39] Y.-K. Lim, Null geodesics in the C metric with a cosmological constant, *Phys. Rev. D* **103**, 024007 (2021).
- [40] T. C. Frost and V. Perlick, Lightlike geodesics and gravitational lensing in the spacetime of an accelerating black hole, *Classical Quantum Gravity* **38**, 085016 (2021).
- [41] A. Ashoorioon, M. B. Jahani Poshteh, and R. B. Mann, Distinguishing a Slowly Accelerating Black Hole by Differential Time Delays of Images, *Phys. Rev. Lett.* **129**, 031102 (2022).
- [42] A. Grenzebach, V. Perlick, and C. Lämmerzahl, Photon regions and shadows of accelerated black holes, *Int. J. Mod. Phys. D* **24**, 1542024 (2015).
- [43] M. Zhang and J. Jiang, Shadows of accelerating black holes, *Phys. Rev. D* **103**, 025005 (2021).
- [44] M. Appels, R. Gregory, and D. Kubiznak, Thermodynamics of Accelerating Black Holes, *Phys. Rev. Lett.* **117**, 131303 (2016).
- [45] A. Anabalón, M. Appels, R. Gregory, D. Kubizňák, R. B. Mann, and A. Ovgün, Holographic thermodynamics of accelerating black holes, *Phys. Rev. D* **98**, 104038 (2018).
- [46] A. Anabalón, F. Gray, R. Gregory, D. Kubizňák, and R. B. Mann, Thermodynamics of charged, rotating, and accelerating black holes, *J. High Energy Phys.* **04** (2019) 096.
- [47] A. Anabalón, S. Brenner, G. Giribet, and L. Montecchio, Closer look at black hole pair creation, *Phys. Rev. D* **104**, 024044 (2021).
- [48] V. Pravda and A. Pravdova, Coaccelerated particles in the C metric, *Classical Quantum Gravity* **18**, 1205 (2001).
- [49] W. Kinnersley and M. Walker, Uniformly accelerating charged mass in general relativity, *Phys. Rev. D* **2**, 1359 (1970).
- [50] W. Bonnor, The sources of the vacuum c -metric, *Gen. Relativ. Gravit.* **15**, 535 (1983).
- [51] J. Bičák and B. Schmidt, Asymptotically flat radiative space-times with boost-rotation symmetry: The general structure, *Phys. Rev. D* **40**, 1827 (1989).
- [52] A. Chamblin, Capture of bulk geodesics by brane world black holes, *Classical Quantum Gravity* **18**, L17 (2001).
- [53] V. Pravda and A. Pravdová, On the spinning c -metric, in *Gravitation: Following The Prague Inspiration: A Volume in Celebration of the 60th Birthday of Jirí Bičák* (World Scientific, Singapore, 2002), pp. 247–262.
- [54] Y.-K. Lim, Geodesic motion in the vacuum C metric, *Phys. Rev. D* **89**, 104016 (2014).
- [55] T. Johannsen, A. E. Broderick, P. M. Plewa, S. Chatzopoulos, S. S. Doeleman, F. Eisenhauer, V. L. Fish, R. Genzel, O. Gerhard, and M. D. Johnson, Testing General Relativity with the Shadow Size of Sgr A*, *Phys. Rev. Lett.* **116**, 031101 (2016).
- [56] A. Boehle, A. Ghez, R. Schödel, L. Meyer, S. Yelda, S. Albers, G. Martinez, E. Becklin, T. Do, J. Lu *et al.*, An improved distance and mass estimate for Sgr A* from a multistar orbit analysis, *Astrophys. J.* **830**, 17 (2016).
- [57] A. Hees *et al.*, Testing General Relativity with Stellar Orbits Around the Supermassive Black Hole in Our Galactic Center, *Phys. Rev. Lett.* **118**, 211101 (2017).
- [58] M. Demianski and M. Francaviglia, Separability structures and Killing-Yano tensors in vacuum type-d space-times without acceleration, *Int. J. Theor. Phys.* **19**, 675 (1980).
- [59] O. J. Dias and J. P. Lemos, Pair of accelerated black holes in an anti-de Sitter background: The AdS C metric, *Phys. Rev. D* **67**, 064001 (2003).
- [60] J. Podolsky and J. B. Griffiths, Uniformly accelerating black holes in a de Sitter universe, *Phys. Rev. D* **63**, 024006 (2000).
- [61] J. Podolsky, Accelerating black holes in anti-de Sitter universe, *Czech. J. Phys.* **52**, 1 (2002).
- [62] Y. Chen, Y.-K. Lim, and E. Teo, New form of the C metric with cosmological constant, *Phys. Rev. D* **91**, 064014 (2015).
- [63] J. B. Griffiths and J. Podolský, A new look at the Plebański–Demiański family of solutions, *Int. J. Mod. Phys. D* **15**, 335 (2006).
- [64] N. Cruz, M. Olivares, and J. R. Villanueva, The geodesic structure of the Schwarzschild anti-de Sitter black hole, *Classical Quantum Gravity* **22**, 1167 (2005).
- [65] M. Jaklitsch, C. Hellaby, and D. Matravers, Particle motion in the spherically symmetric vacuum solution with positive cosmological constant, *Gen. Relativ. Gravit.* **21**, 941 (1989).
- [66] T. Padmanabhan, Cosmological constant: The weight of the vacuum, *Phys. Rep.* **380**, 235 (2003).
- [67] R. Howes, Existence and stability of circular orbits in a schwarzschild field with nonvanishing cosmological constant, *Aust. J. Phys.* **32**, 293 (1979).
- [68] P. Boonserm, T. Ngampitipan, A. Simpson, and M. Visser, Innermost and outermost stable circular orbits in the presence of a positive cosmological constant, *Phys. Rev. D* **101**, 024050 (2020).
- [69] F. Eisenhauer, R. Schödel, R. Genzel, T. Ott, M. Tecza, R. Abuter, A. Eckart, and T. Alexander, A geometric determination of the distance to the galactic center, *Astrophys. J. Lett.* **597**, L121 (2003).